

# Seismic peak amplitude as a predictor of TOC content in shallow marine sediments

Arthur Ayres Neto<sup>1</sup> · Bruno Bourguignon Mota<sup>1</sup> · André Luiz Belem<sup>2</sup> · Ana Luiza Albuquerque<sup>2</sup> · Ramsés Capilla<sup>3</sup>

Received: 11 January 2016 / Accepted: 6 April 2016 / Published online: 13 April 2016  
© Springer-Verlag Berlin Heidelberg 2016

**Abstract** Acoustic remote sensing is a highly effective tool for exploring the seafloor of both deep and shallow marine settings. Indeed, the acoustic response depends on several physicochemical factors such as sediment grain size, bulk density, water content, and mineralogy. The objective of the present study is to assess the suitability of seismic peak amplitude as a predictor of total organic carbon (TOC) content in shallow marine sediments, based on data collected in the Cabo Frio mud belt in an upwelling zone off southeastern Brazil. These comprise records of P-wave velocity ( $V_P$ ) along 680 km of high-resolution single-channel seismic surveys, combined with analyses of grain size, wet bulk density, absolute water content and TOC content for four piston-cores. TOC contents of sediments from 13 box-cores served to validate the methodology. The results show well-defined positive correlations between TOC content and mean grain size (phi scale) as well as absolute water content, and negative correlations with  $V_P$ , wet bulk density, and acoustic impedance. These relationships yield a regression equation by which TOC content can be satisfactorily predicted on the basis of acoustic impedance for this region:  $y = -4.84 \ln(x) + 40.04$ . Indeed, the derived TOC contents differ by only 5% from those determined by geochemical analysis. After appropriate calibration, acoustic

impedance can thus be conveniently used as a predictor of large-scale spatial distributions of organic carbon enrichment in marine sediments. This not only contributes to optimizing scientific project objectives, but also enhances the cost-effectiveness of marine surveys by greatly reducing the ship time commonly required for grid sampling.

## Introduction

Geoacoustic characterization of near-surface marine sediments has received increasing attention worldwide during the last decades since pioneer research dating back to the 1980s. In general, those studies were aimed at creating a framework correlation between acoustic attributes and sedimentological parameters to achieve a more quantitative characterization of the seafloor in geological, environmental and geotechnical terms, today commonly coupled with geoacoustic modeling exercises (e.g., Hamilton 1980; Hamilton and Bachman 1982; Richardson and Briggs 1993, 2002; Ayres and Theilen 1999; Bartholomä 2006; Cruz et al. 2013; Mendoza et al. 2014; Wöfl et al. 2014; Daniell et al. 2015). The main acoustic attributes used for this characterization are the P-wave velocity ( $V_P$ ), wet bulk density ( $\rho$ ) and acoustic impedance ( $Z$ ), the latter defined as the product of the former two parameters:

$$Z = \rho V_P \quad (1)$$

Several sedimentological and biological factors (grain size, porosity, water content, compaction, contact between grains, bioturbation, etc.) as well as operational factors (signal intensity, beam angle and frequency) control the P-wave responses within sediments simultaneously and on different scales (Collins et al. 1996; Jackson and Richardson 2007).

✉ Arthur Ayres Neto  
aayres@id.uff.br

<sup>1</sup> Geology and Geophysics Department, Universidade Federal Fluminense, Av. General Milton Tavares de Souza, s/n Gragoatá, 24322-095 Niterói, RJ, Brazil

<sup>2</sup> Geochemistry Department, Universidade Federal Fluminense, Outeiro São João Baptista s/n Centro, Niterói, RJ, Brazil

<sup>3</sup> Petrobras Research Center (CENPES), Av. Horácio Macedo 950, Cidade Universitária, 21941-915 Rio de Janeiro, RJ, Brazil

Operating parameters are relatively easy to control and, once set, must remain constant throughout the survey. A change in these settings would result in a change in the acoustic response of the sediment, thereby preventing meaningful comparisons between different materials. In contrast, sedimentological factors vary quite randomly. Even within the same depositional environment, sediments can show heterogeneities on scales ranging from millimeters to tens of meters (Preston et al. 1997). Such heterogeneities are generated from the start of the sedimentation process by, for example, the deposition of larger objects (e.g., shells) within a finer matrix and changes in the grain fabric, which together define the porosity and gradational layering caused by variations in energy in the course of deposition (Briggs and Richardson 1997). The overall acoustic response arises from a combination of these factors and, therefore, changes in any of these parameters would be reflected in the acoustic signature of the sediment.

Acoustic geophysical methodologies (echosounding, side-scan sonography, high-resolution seismic profiling, and sediment acoustic classification) are key tools in modern marine research, requiring a sound knowledge of interrelations between seafloor acoustic and physicochemical properties. Particularly today, these are strategic elements in developing geoaoustic models supporting, for example, subsea oil and gas exploration, offshore mining, and harbor engineering, as well as environmental impact assessments of these and other human activities. Notable applications include regional-scale assessments of methane dynamics (e.g., Mogollón et al. 2013) and organic carbon enrichment (e.g., Leipe et al. 2011), one advantage being a reduction in fieldwork and laboratory costs.

Within this context, the present study explores the relationship between sedimentary organic matter and acoustic response of near-surface marine sediments at the western boundary of the Cabo Frio upwelling system (CFUS) of southeastern Brazil (Fig. 1). In this region, productivity and sedimentation patterns are controlled by synergetic oceanographic processes resulting in a variety of upwelling areas on the continental shelf (Belem et al. 2013), and promoting accumulation of organic matter-enriched sediments (Sanders et al. 2014). In the CFUS, sedimentary organic matter originates from both marine and terrigenous sources (Yoshinaga et al. 2008; Albuquerque et al. 2014). Marine sources dominate (Cordeiro et al. 2014; Sanders et al. 2014), rooted mainly in labile marine planktonic debris produced during upwelling events. Thus, a strong correlation between primary productivity and sediment total organic carbon (TOC) content can be expected (see, for example, Freudenthal et al. 2001). Terrigenous sources comprise continentally derived higher plant material delivered by riverine input and subsequently reworked by southward-flowing coastal plumes to eventually be dispersed along the Cabo Frio continental shelf. Cruz et al. (2013) reported similarities in physical sediment properties between the inner and outer shelf sectors, despite energy

conditions being higher on the inner shelf. Mendoza et al. (2014) used acoustic data coupled with physicochemical sediment characteristics (grain size, TOC, sedimentation rates and absolute ages) to investigate the millennial-scale evolution of the Cabo Frio shelf deposit.

The main objective of the present study is to explore interrelationships between TOC contents and the propagation velocity of P-waves ( $V_p$ ), wet bulk density ( $\rho$ ), and acoustic impedance ( $Z$ ) of shallow marine sediments in the CFUS. Moreover, it assesses whether acoustic impedance can serve to estimate large-scale spatial distribution patterns of sediment organic carbon in the region.

## Physical setting

The study area is located off the city of Cabo Frio in water depths of 80 to 140 m at the confluence of the eastern and southern coastal sectors of the state of Rio de Janeiro (Fig. 1). Coastal upwelling brings deep, cold and nutrient-rich water to the ocean surface and/or photic zone from early spring to late summer (Carbonel and Valentin 1999; Belem et al. 2013), favoring the production of organic matter due to nutrient availability. Upwelling is forced primarily by the NE coastal wind regime, in combination with morphological features and the meso-scale dynamics of the Brazil Current, which promotes inflow of South Atlantic Central Water onto the continental shelf (Rodrigues and Lorenzetti 2001; Castelao and Barth 2006; Belem et al. 2013).

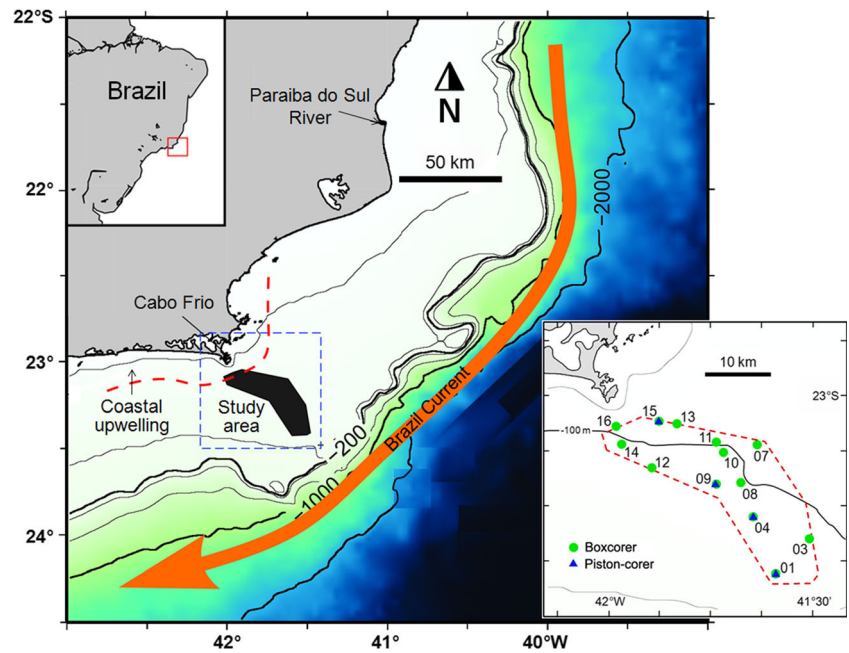
The inner shelf is dominated by terrigenous sediments and the outer shelf primarily by carbonate sediments (Figueiredo and Madureira 2004). Due to the confluence of northerly and southerly wind-driven coastal currents, however, an extensive accumulation of muddy terrigenous sediments extends seaward up to the shelf break where carbonate sands predominate (Dias et al. 1982; Fig. 1). This mud is supplied mainly by small local rivers, but also by the Paraíba River (located approx. 180 km north of Cabo Frio) and Guanabara Bay (located 150 km to the west; Knoppers and Moreira 1990; Albuquerque et al. 2016).

## Materials and methods

The seismic survey was conducted in spring 2009 using a Geoaoustics Geopulse 3.5 kHz single-channel chirp system and covering 680 km. Positioning was by means of a DGPS CNAV 2000 system.

Seismic peak amplitude was determined using the Kingdom Suite software (IHS, Taiwan) after the first acoustic reflection of the seabed had been mapped (Fig. 2a). The values were then filtered using a moving average of ten seismic shots. As an example, Fig. 2b shows the original peak amplitude

**Fig. 1** Geographic locations of the study area (black Cabo Frio mud belt), and the box- and piston-cores (see Table 1)



values and the filtered data from seismic line 19. Due to the high quality of the seismic data and restriction to the uppermost sediment layer, no seismic post-processing techniques (stacking, muting, statics correction, velocity analysis, migration, etc.) were applied.

Seabed samples were collected with a 6-m-long piston-corer and a 50×50 cm box-corer at 17 sites chosen on the basis

of different echo-characters observed in the seismic data (cf. geographic coordinates in Table 1, and locations in Fig. 1). In the laboratory, the four piston-cores were profiled by means of a multi-sensor core logger to obtain  $V_p$  and wet bulk density values at 1 cm intervals (Schultheiss and Weaver 1992). The cores were split in half, and subsamples were taken every 5 cm from one half for grain size analyses of sand (−1 to 4 phi), silt

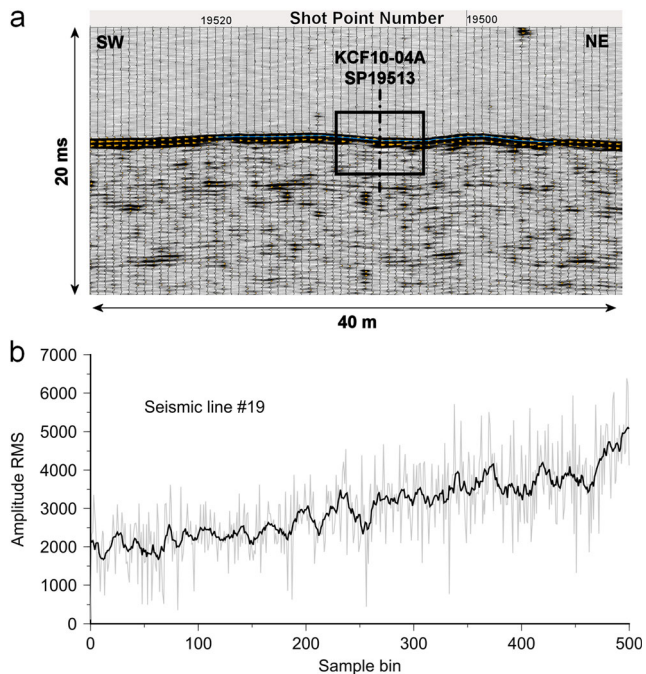


**Fig. 2** a Example of a seismic line (FEC\_00026) with interpreted seabed reflector (blue line). Yellow Wiggle traces. Box Traces used to calculate average amplitude values in the vicinity of core KCF10-04A. b Seismic peak amplitude values (gray line) and filtered data (black line) of seabed reflector from seismic line 19

**Table 1** Geographic coordinates of piston- and box-core sampling stations

Core	Lat. (S)	Long. (W)
<b>Piston-corer</b>		
KCF10-01A	23°40'39"	41°59'00"
KCF10-04A	23°28'04"	42°04'47"
KCF10-09A	23°20'14"	42°14'01"
KCF10-15C	23°06'26"	42°28'01"
<b>Box-corer</b>		
BCCF10-01	23°40'39"	41°59'00"
BCCF10-02	23°32'53"	41°51'17.5"
BCCF10-04	23°28'04"	42°04'47"
BCCF10-07	23°11'21"	42°03'52"
BCCF10-08	23°20'22"	42°07'51"
BCCF10-09	23°20'14"	42°14'01"
BCCF10-10	23°13'24"	42°12'01"
BCCF10-11	23°10'54"	42°13'56"
BCCF10-12	23°16'40"	42°29'36"
BCCF10-13	23°06'51"	42°23'17"
BCCF10-14	23°11'03"	42°37'10"
BCCF10-15	23°06'26"	42°28'01"
BCCF10-16	23°07'07"	42°38'10"

(4–9 phi) and clay (<9 phi), as well as absolute water content (weight%). TOC contents (weight%) of bulk sediments in the piston-cores were extracted from Mendoza et al. (2014). TOC contents of the 13 box-cores were determined as described by Mendoza et al. (2014) for the piston-cores.

In a preliminary check for the purpose of the present study, TOC contents were converted into TOC concentrations (mass per unit volume,  $\text{g cm}^{-3}$ ) following the standard approach described in Flemming and Delafontaine (2000). Table 2 summarizes the correlation coefficients (R) between TOC contents/concentrations and some relevant physical parameters. Coefficients for TOC concentrations were found to be considerably lower than those for TOC contents. This is not surprising, seeing that interrelations between TOC contents and concentrations are commonly not straightforward (see Flemming and Delafontaine 2000, 2016; Leipe et al. 2011). For this reason, the present study focuses only on TOC contents.

## Results

### TOC vs. physical properties

**TOC vs. mean grain size** Piston-cores KCF10-01A and KCF10-15C, at the southeastern and northwestern limits of the study area, respectively, have relatively high sand contents with mean grain sizes typically ranging from 6 phi (medium silt) to 3.7 phi (very fine sand). In contrast, piston-cores KCF10-04A and KCF10-09A from the central part of the study area are characterized by silty clays with mean grain sizes of usually >6 phi (medium to fine silt). In general, mean grain size tends to decrease slightly with depth in all four cores.

TOC contents range from 0.16–3.28% (cf. Mendoza et al. 2014), the highest values being observed in cores KCF10-04A and KCF10-09A (means of 1.94% and 2.77%, respectively) comprising mainly finer sediments. In contrast, cores with coarser mean grain sizes (lower mean phi values) have lower mean TOC contents (1.18% for core KCF10-01A and 1.08% for core KCF10-15C). For all cores combined, TOC contents correlate positively with mean grain size expressed in phi, the correlation coefficient being  $R=0.79$  (Fig. 3a). Note that this correlation would be negative if the mm-scale were used.

**TOC vs. P-wave velocity**  $V_p$  values range between 1,401 and 1,763  $\text{m s}^{-1}$ , with highest values in cores KCF10-15C and KCF10-01A. Figure 3b shows that P-wave velocity increases as TOC content decreases ( $R=-0.72$ ).

**TOC vs. wet bulk density** The relationship between wet bulk density ( $\rho$ ) and TOC shows the same trend as that observed for P-wave velocity, with  $\rho$  inversely correlated with TOC content ( $R=-0.75$ , Fig. 3c). Wet bulk density values range from 1.33 to 2.44  $\text{g cm}^{-3}$ , with highest values in cores KCF10-01A and KCF10-15C.

**TOC vs. acoustic impedance**  $Z$  values range from 2,135 to 3,364  $\text{N s m}^{-3}$ , exhibiting a clear negative correlation with TOC content ( $R=-0.77$ , Fig. 3d). This correlation is slightly more pronounced than those observed for TOC versus P-wave velocity and wet bulk density. The regression equation for TOC content ( $y$ ) versus acoustic impedance ( $x$ ) is:

$$y = -4.84\ln(x) + 40.04 \quad (2)$$

**TOC vs. absolute water content** The absolute water contents ( $W$ ) of sediments in the four piston-cores vary in the range of approx. 20 to 60%, with highest values in cores KCF10-04A and KCF10-09A.  $W$  shows a strong positive correlation with TOC content ( $R=0.81$ , Fig. 4).

### Validation of derived TOC contents

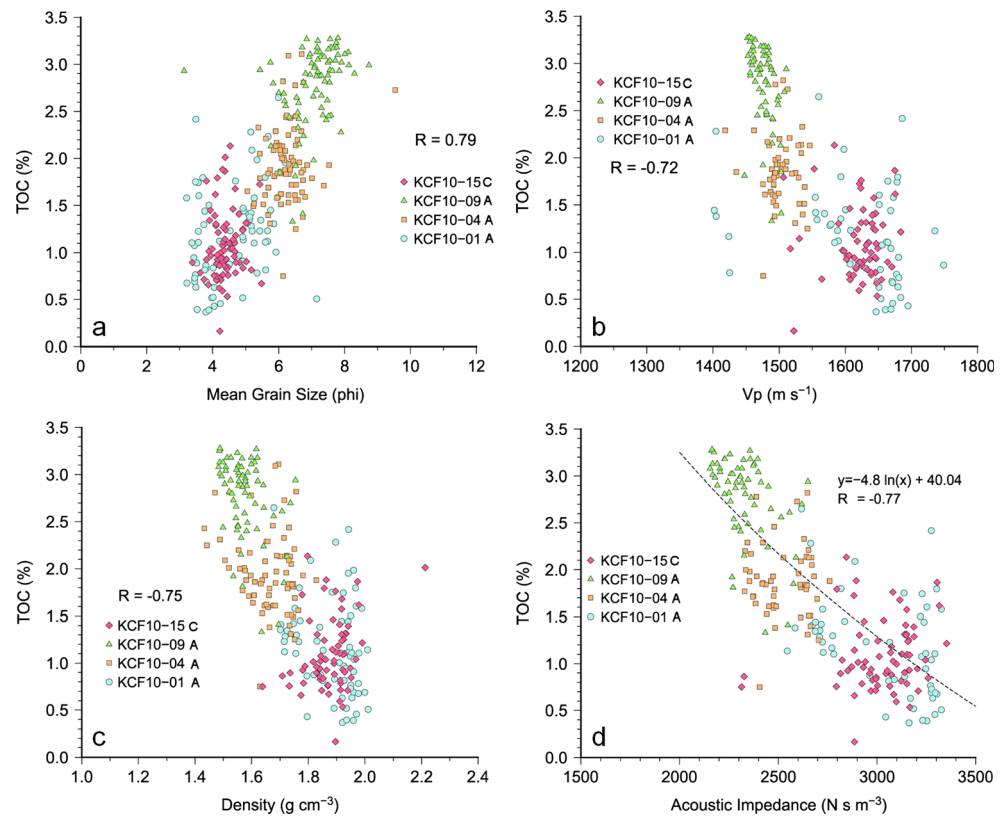
Figure 5a shows the relationship between the average seismic peak amplitude and the average acoustic impedance for the piston-core locations. The amplitude was calculated by averaging the peak amplitude of the ten traces closest to the position of each core, i.e., five on each side (cf. Fig. 2a), representing a distance of 4.1 m for the reflector corresponding to the seafloor. Similarly, the acoustic impedance was calculated by averaging the values for the upper 25 cm of each core, which corresponds roughly to the seismic resolution of the 3.5 kHz signal used for the survey. The regression equation for acoustic impedance ( $y$ ) versus seismic peak amplitude ( $x$ ) is reported below, with the standard deviations for average acoustic impedance and average amplitude of each of the four data points given in Table 3:

$$y = 0.156x + 1,888 \quad (3)$$

**Table 2** Correlation coefficients for TOC contents (weight %) and concentrations ( $\text{g cm}^{-3}$ ) versus mean grain size (phi), P-wave velocity ( $V_p$ ), wet bulk density ( $\rho$ ), acoustic impedance ( $Z$ ), and absolute water content ( $W$ )

	TOC vs. phi	TOC vs. $V_p$	TOC vs. $\rho$	TOC vs. $Z$	TOC vs. $W$
(%)	0.79	-0.72	-0.75	-0.77	0.81
( $\text{g cm}^{-3}$ )	0.48	-0.13	-0.12	-0.13	0.55

**Fig. 3** Cross-plots between **a** mean grain size ( $\phi$ ), **b**  $V_p$ , **c** wet bulk density, **d** acoustic impedance and TOC content (piston-cores,  $n=310$ )



A combination of the regression equations calculated for the relationships reported in Figs. 3d and 5a served to “transform” the peak amplitude values into TOC contents for seafloor sediments in the study area. This enabled generating a large-scale spatial TOC map by extrapolating TOC contents laterally between closely spaced seismic profiles (see below).

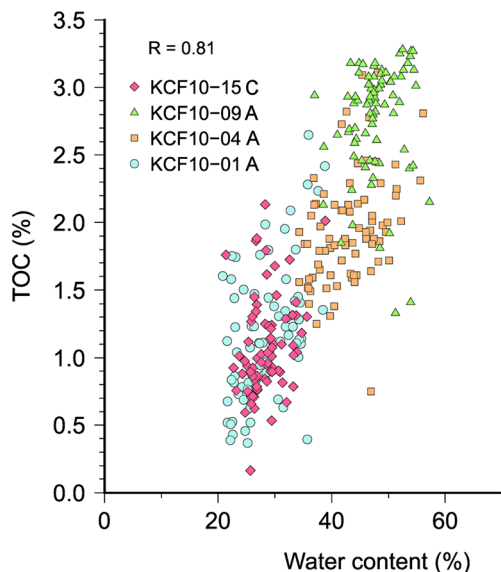


**Fig. 4** Cross-plot between absolute water content and TOC content (piston-cores,  $n=310$ )

To validate the relationship between measured TOC contents and acoustic impedance recorded in the four piston-cores (cf. Fig. 3d), TOC contents determined by chemical analysis are plotted against TOC contents derived from seismic peak amplitude for the 13 box-cores in Fig. 5b. The variations between values listed in Table 4 range from 14–35% (mean difference of 14%), with the most prominent differences being observed at stations where TOC contents are above 2% according to chemical analysis. The scatter diagram in Fig. 5b evidences a strong linear correlation ( $R=0.82$ ) between observed (chemical analysis) and predicted (seismic peak amplitude) TOC contents. The regression equation indicates that a correction of only 5% is needed to align the observed and predicted datasets. Such deviations may have several causes, including the choice of gridding algorithm, the resolution of petrophysical measurements ( $V_p$ , wet bulk density), the quality of seismic data, the horizontal resolution of core locations and, last but not least, the choice of chemical analysis procedures (e.g., see Passos et al. 2016).

The scatter diagram of Fig. 3a reveals that sediments with TOC contents  $<2\%$  are characteristically coarser than 6  $\phi$ , i.e., they have higher proportions of sandy material. For sandier sediments (mean grain sizes of 3–6  $\phi$ ), acoustic impedance varies roughly between 2,500 and 3,350  $N s m^{-3}$  (approx. 34%; Fig. 6). The range is narrower for finer sediments (mean grain size of 6–9  $\phi$ ), where acoustic impedance varies from 2,130 to 2,500  $N s m^{-3}$  (approx. 17%).

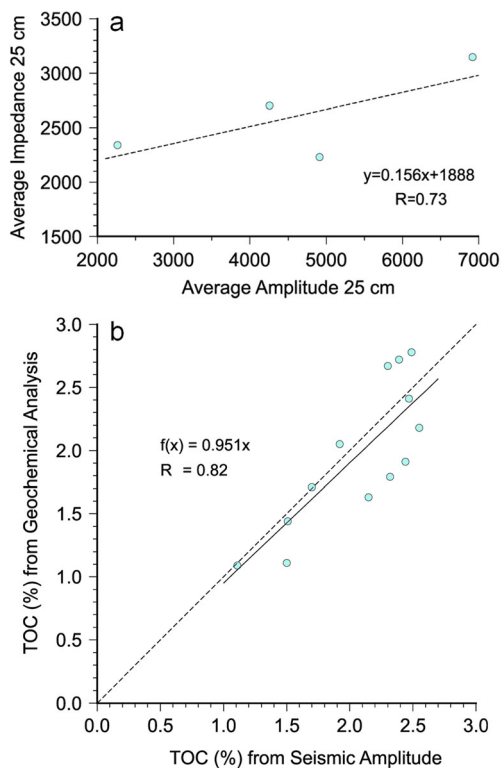


**Fig. 5** **a** Average peak seismic amplitude vs. average acoustic impedance at piston-core locations. **b** TOC content obtained from chemical analysis of box-core samples vs. TOC content derived from seismic peak amplitude at the same locations

Figure 7 shows the large-scale TOC spatial distribution in the Cabo Frio mud belt as derived from seafloor peak amplitude. To the south, there is a distinct demarcation of a main, organically enriched zone (TOC values exceeding 2%) aligned roughly NW–SE. Along the northern and eastern fringes, TOC contents are below 2%.

## Discussion

The present results show that the sediments of the study area can be subdivided into two groups according to their physical characteristics. At the SE and NW extremes of the study area (cores KCF10-01A and KCF10-15C), the sediments have higher sand contents, and consequently  $V_B$  wet bulk density

**Table 3** Standard deviations (SD) for each of the four data points shown in Fig. 5a

Piston-core	SD Average amplitude	SD Average impedance
KCF10-01A	904	58
KCF10-04A	1,263	62
KCF10-09A	2,013	58
KCF10-15C	1,397	37

and impedance values are higher and TOC contents are lower. In the central study area (cores KCF10-04A and KCF10-09A) where sand contents are lower (cf. higher silt and clay contents),  $V_B$  wet bulk density and impedance values are lower and TOC contents are correspondingly higher.

The data clearly reveal that increasing organic matter enrichment is accompanied by progressive reductions in the P-wave velocity and wet bulk density of sediments (cf. Figs. 3b, c). This can be explained by organic matter being closely tied to the finest silts and clays. The negative electrostatic charge of clay surfaces and dissociation of organic acids cause water to be bound within the sediment (Mayer et al. 2002). Moreover, the water adsorbed by clay minerals and organic matter leads to an increase in sediment pore pressure, which inhibits compaction and results in less dense sediments. In turn, these are acoustically less reflective because the impedance contrast relative to seawater is lower than for denser sediments.

The reflection coefficient (RC) is the controlling property of acoustic energy transmission across a boundary, and is defined by the following relationship for normally incident acoustic waves:

$$RC = \frac{(z_2 - z_1)}{(z_2 + z_1)} \quad (4)$$

Nonetheless, compared to typical seafloor sediments where a higher impedance contrast with seawater is observed, very low density sediments ( $<1.2 \text{ g cm}^{-3}$ ) can hamper bottom detection by echosounders and high-resolution seismic systems (Van Walree et al. 2005). This is the case for estuaries and enclosed bays, which typically contain very high amounts of organic matter and where precise determination of water depth is critical for safe navigation. Figure 3d confirms this observation—the higher the acoustic impedance, the lower is the TOC content.

Knight et al. (1998) demonstrated that small variations in P-wave velocity are most likely to result from heterogeneities in saturation. Under conditions of capillary equilibrium, local lithological heterogeneities (primarily due to changes in mineralogy and grain size) can cause different saturations, depending on their porosity and permeability. Cruz et al. (2013) made similar observations (although with lower correlation coefficients) for very shallow box-core samples collected in the present study area. For surface sediments of the Arkona Basin in the Baltic Sea, Endler et al. (2015) reported a similar trend of increasing  $V_P$  with decreasing TOC content (percentage loss on ignition divided by 2.8), as well as a negative correlation between TOC content and acoustic impedance. In the Santos Basin of Brazil, Ayres Neto et al. (2013) found better correlation between different physical parameters and acoustic impedance than with  $V_P$  and wet bulk density. The same cost-effective approach combining large-scale seismic surveying and ground-truth coring enabled Mendonça et al. (2014) to highlight the importance of

**Table 4** Comparison between TOC contents calculated by seismic amplitude and those determined by chemical analysis

Box-core	TOC by amplitude (%)	TOC by chemical analysis (%)	Difference (%)
BCCF10-01	1.9	2.1	-6
BCCF10-02	1.5	1.1	35
BCCF10-04	2.6	2.2	17
BCCF10-07	1.7	1.7	-1
BCCF10-08	2.4	2.7	-12
BCCF10-09	2.5	2.8	-10
BCCF10-10	2.3	1.8	29
BCCF10-11	2.2	1.6	32
BCCF10-12	2.4	1.9	28
BCCF10-13	1.5	1.4	5
BCCF10-14	2.3	2.7	-14
BCCF10-15	1.1	1.1	2
BCCF10-16	2.5	2.4	2
Mean difference			14

hydroelectric reservoir sediments as organic matter sinks. In the present study, the large-scale TOC spatial distribution in the Cabo Frio mud belt was successfully derived from seafloor peak amplitude (Fig. 7).

The relationship between mean grain size and acoustic impedance (Fig. 6) suggests that the main factor controlling the latter, and therefore peak amplitude, is the content of coarse material in the sediment. Coarse sediments in marine environments are usually composed of quartz grains and bioclasts, neither of which have the electrostatic properties of clay minerals. As a consequence, they are unable to adhere organic matter to their surfaces. Due to this affinity of organic matter to clay minerals, TOC enrichment is commonly higher in fine-grained sediments deposited in low-energy environments. Such sediments inherently have a lower acoustic reflectivity. Future research should therefore focus on a more detailed evaluation of the impact of sediment composition on P-wave reflectivity.

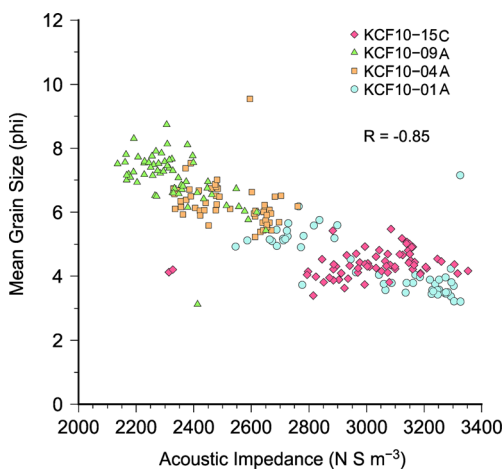


**Fig. 6** Cross-plot between sediment mean grain size (phi) and acoustic impedance (piston-corers,  $n=310$ )

### Conclusions

The present study investigated interrelations between TOC content and the acoustic response of shallow marine sediments in the Cabo Frio mud belt of southeastern Brazil. Acoustic impedance and seismic peak amplitude are strongly affected by coarse sediment particle content. TOC content is controlled by its known affinity for clay and fine silt fractions. The main conclusions are:

- After appropriate calibration using a small number of reference cores, TOC contents can reliably be predicted by seismic peak amplitude.
- The sensitivity of the method decreases as TOC contents reach values above approx. 2% in fine-grained sediments; the reflectivity of the seismic pulse then becomes very

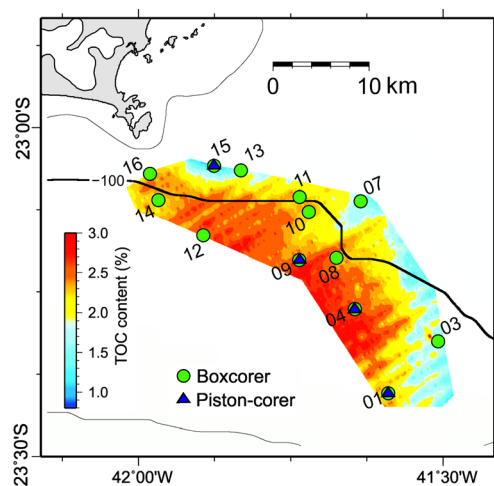


**Fig. 7** Spatial distribution of TOC content in the study area based on seismic peak amplitude

low and hence unsuitable for deciphering more subtle trends in organic enrichment.

- The study deals with sediments of an upwelling zone; the approach should be tested in other settings marked by strong organic carbon gradients.
- The application of this integrative approach combining seismic surveys and ground-truth coring not only facilitates meeting scientific project objectives, but also increases the cost-effectiveness of the operations by greatly reducing the ship time commonly required for grid sampling.

**Acknowledgements** This work was supported by grant #0050.0048388.08.9 from the Geochemistry Network of the Petroleum National Agency and Petrobras, in cooperation with Universidade Federal Fluminense, Brazil. The authors wish to thank three reviewers and the editors for their valuable contributions to this paper.

#### Compliance with ethical standards

**Conflict of interest** The authors declare that there is no conflict of interest with third parties.

## References

- Albuquerque ALS, Belem AL, Zuluaga FJ, Cordeiro LG, Mendoza U, Knoppers BA, Gurgel MH, Meyers PA, Capilla R (2014) Particle fluxes and bulk geochemical characterization of the Cabo Frio upwelling system in Southeastern Brazil: sediment trap experiments between spring 2010 and summer 2012. *Anais Acad Bras Ciências* 86(2):601–620
- Albuquerque ALS, Meyers P, Belem AL, Turcq B, Sifeddine A, Mendoza U, Capilla R (2016) Mineral and elemental indicators of post-glacial changes in sediment delivery and deposition under a western boundary upwelling system (Cabo Frio, Southeastern Brazil). *Palaeogeogr Palaeoclimatol Palaeoecol* 445:72–82
- Ayres A, Theilen F (1999) Relationship between seismic velocities and geological and geotechnical properties of near surface marine sediments of the continental slope of the Barents Sea. *Geophys Prospect* 47(4):431–441
- Ayres Neto A, Mendes JNT, Souza JMG, Redusino M Jr, Pontes RLB (2013) Geotechnical influence on the acoustic properties of marine sediments of the Santos Basin, Brazil. *Mar Georesour Geotechnol* 31:125–136
- Bartholomä A (2006) Acoustic bottom detection and seabed classification in the German Bight, southern North Sea. *Geo-Mar Lett* 26: 177–184. doi:10.1007/s00367-006-0030-6
- Belem AL, Castelao RM, Albuquerque AL (2013) Controls of subsurface temperature variability in a western boundary upwelling system. *Geophys Res Lett* 40:1362–1366
- Briggs KB, Richardson MD (1997) Small-scale fluctuations in acoustic and physical properties in surficial carbonate sediments and their relationship to bioturbation. *Geo-Mar Lett* 17:306–315. doi:10.1007/s003670050042
- Carbonel C, Valentin JL (1999) Numerical modelling of phytoplankton bloom in the upwelling ecosystem of Cabo Frio (Brazil). *Ecol Model* 116:135–148
- Castelao RM, Barth JA (2006) Upwelling around Cabo Frio, Brazil: the importance of wind stress curl. *Geophys Res Lett* 33, L03602. doi:10.1029/2005GL025182
- Collins WT, Gregory RS, Anderson JT (1996) A digital approach to seabed classification. *Sea Technol* 37(8):83–87
- Cordeiro LGMS, Belem AL, Bouloubassi I, Rangel B, Sifeddine A, Capilla R, Albuquerque ALS (2014) Reconstruction of southwestern Atlantic sea surface temperatures during the last Century: Cabo Frio continental shelf (Brazil). *Palaeogeogr Palaeoclimatol Palaeoecol* 415:225–232
- Cruz APS, Barbosa CF, Ayres Neto A, Albuquerque ALS (2013) Physical and geochemical properties of centennial marine sediments of the continental shelf of southeast Brazil. *Geochim Bras* 27:1–12
- Daniell J, Siwabessy J, Nichol S, Brooke B (2015) Insights into environmental drivers of acoustic angular response using a self-organising map and hierarchical clustering. *Geo-Mar Lett* 35:387–403. doi:10.1007/s00367-015-0415-5
- Dias GTM, Palma JJC, Ponzi VRA (1982) Organic matter in Quaternary sediments of the continental margin between Rio de Janeiro and Guarapari (in Portuguese). LAGEMAR/PETROBRAS/CENPES Report, Rio de Janeiro, Brazil
- Endler M, Endler R, Bobertz B, Leipe T, Arz HW (2015) Linkage between acoustic parameters and seabed sediment properties in the south-western Baltic Sea. *Geo-Mar Lett* 35:145–160. doi:10.1007/s00367-015-0397-3
- Figueiredo AG Jr, Madureira LSP (2004) Topography, composition, reflectivity of the seafloor and identification of sedimentary provinces along the southeast coast of Brazil (in Portuguese). Série Documentos 443, Técnicos do Programa REVIZEE Score-Sul, Instituto Oceanográfico, USP, São Paulo
- Flemming BW, Delafontaine MT (2000) Mass physical properties of muddy intertidal sediments: some applications, misapplications and non-applications. *Cont Shelf Res* 20:1179–1197. doi:10.1016/S0278-4343(00)00018-2
- Flemming BW, Delafontaine MT (2016) Mass physical sediment properties. In: Kennish MJ (ed) *Encyclopedia of Estuaries*. Springer, Dordrecht, pp 419–432. doi:10.1007/978-94-017-8801-4\_350
- Freudenthal T, Wagner T, Wenzhöfer F, Zabel M, Wefer G (2001) Early diagenesis of organic matter from sediments of the eastern subtropical Atlantic: evidence from stable nitrogen and carbon isotopes. *Geochim Cosmochim Acta* 65(11):1795–1808
- Hamilton EL (1980) Geoacoustic modeling of the sea floor. *J Acoust Soc Am* 68:1313–1340
- Hamilton EL, Bachman RT (1982) Sound velocity and related properties of marine sediments. *J Acoust Soc Am* 72:1891–1904
- Jackson DR, Richardson MD (2007) *High-frequency seafloor acoustics*. Springer, New York
- Knight R, Dvorkin J, Nur A (1998) Acoustic signatures of partial saturation. *Geophysics* 63:132–138
- Knoppers B, Moreira PF (1990) Suspended material and phytoplankton succession in Guarapina Lagoon, RJ (in Portuguese). *Acta Limnol Bras* 3:291–317
- Leipe T, Tauber F, Vallius H, Virtasalo J, Uściniowicz S, Kowalski N, Hille S, Lindgren S, Myllyvirta T (2011) Particulate organic carbon (POC) in surface sediments of the Baltic Sea. *Geo-Mar Lett* 31:175–188. doi:10.1007/s00367-010-0223-x
- Mayer L, Benninger M, Bocka D, DeMaster Q, Roberts C, Martense D (2002) Mineral associations and nutritional quality of organic matter in shelf and upper slope sediments off Cape Hatteras, USA: a case of unusually high loadings. *Deep-Sea Res II* 49:4587–4597
- Mendonça R, Kosten S, Sobek S, Cole JJ, Bastos AC, Albuquerque AL, Cardoso SJ, Roland F (2014) Carbon sequestration in a large hydroelectric reservoir: an integrative seismic approach. *Ecosystems* 17(3):430–441

- Mendoza U, Ayres Neto A, Abuchacra RC, Barbosa CF, Figueiredo AG Jr, Gomes MC, Belem AL, Capilla R, Albuquerque ALS (2014) Geoacoustic character, sedimentology and chronology of a cross-shelf Holocene sediment deposit off Cabo Frio, Brazil (southwest Atlantic Ocean). *Geo-Mar Lett* 34:297–314. doi:10.1007/s00367-014-0370-6
- Mogollón JM, Dale AW, Jensen JB, Schlüter M, Regnier P (2013) A method for the calculation of anaerobic oxidation of methane rates across regional scales: an example from the Belt Seas and The Sound (North Sea–Baltic Sea transition). *Geo-Mar Lett* 33:299–310. doi:10.1007/s00367-013-0329-z
- Passos TRG, Artur AG, Nóbrega GN, Otero XL, Ferreira TO (2016) Comparison of the quantitative determination of soil organic carbon in coastal wetlands containing reduced forms of Fe and S. *Geo-Mar Lett* 36. doi:10.1007/s00367-016-0437-7
- Preston S, Griffiths BS, Young IM (1997) An investigation into sources of soil crack heterogeneity using fractal geometry. *European J Soil Sci* 48:31–37
- Richardson MD, Briggs KB (1993) On the use of acoustic impedance values to determine sediment properties. *Proc Inst Acoust* 15(P2): 15–24
- Richardson MD, Briggs KB (2002) On the use of acoustic impedance values to determine sediment properties. In: Pace NG, Langhorne DN (eds) *Acoustic classification and mapping of the seabed*. Institute of Acoustics, Bath, pp 15–25
- Rodrigues RR, Lorenzetti JA (2001) A numerical study of the effects of bottom topography and coastline geometry on the Southeast Brazilian coastal upwelling. *Cont Shelf Res* 21: 371–394
- Sanders CJ, Caldeira PP, Smoak JM, Ketterer ME, Belem A, Mendoza UM, Cordeiro LGM, Patchneelan SR, Silva-Filho EV, Albuquerque ALS (2014) Recent organic carbon accumulation (~100 years) along the Cabo Frio, Brazil upwelling region. *Cont Shelf Res* 75:68–75
- Schultheiss PJ, Weaver PPE (1992) Multi-sensor core logging for science and industry. *J IEEE* 7:608–613
- Van Walree PA, Tegowski J, Laban C, Simons DG (2005) Acoustic sea-floor discrimination with echo shape parameters: a comparison with ground truth. *Cont Shelf Res* 25:2273–2293
- Wöfl A-C, Lim CH, Hass HC, Lindhorst S, Tosonotto G, Lettmann KA, Kuhn G, Wolff J-O, Abele D (2014) Distribution and characteristics of marine habitats in a subpolar bay based on hydroacoustics and bed shear stress estimates—Potter Cove, King George Island, Antarctica. *Geo-Mar Lett* 34:435–446. doi:10.1007/s00367-014-0375-1
- Yoshinaga MY, Sumida PYG, Wakeham SG (2008) Lipid biomarkers in surface sediments from an unusual coastal upwelling area from the SW Atlantic Ocean. *Org Geochem* 39(10):1385–1399